SCIFED Publishers

Paizullakhanov MS, SF J Material Res Let , 2017, 1 :3

SciFed Materials Research Letters

Review Article Open Access

$BiFeO_3$ Synthesized on the Solar Furnace

[1]Atabayev IG, [*2]Paizullakhanov MS

[*2]*Material science institute, Uzbekistan, Tashkent, Bodomzor street 2-B, Russia*

Abstract

It is shown that ferrite of bismuth synthesized on the basis of precursors - iron and bismuth oxides melted on a solar furnace has a denser structure, a low coefficient of thermal expansion, in comparison with the traditionally synthesized bismuth ferrite.

Introduction

As the analysis shows, the materials of perovskite (Ti (Sr) BaO_3) and pyroxene ($CaMgSi_2O_6$) compositions synthesized from melt in the Big Solar Furnace (BSP) have a stable stable structure and increased mechanical and dielectric properties [1-3]. However, the synthesis of perovskite structures based on bismuth ferrite $BiFeO_3$ with magnetic properties using BSP has not been studied.

Synthesis and properties of bismuth ferrite BiFeO3 are investigated quite widely [1-16]. However, the preparation of a single-phase sample of $BiFeO_3$ still presents a serious problem. For example, a material synthesized from a mixture of Bi_2O_3 + Fe_2O_3 always contains impurities $Bi_{25}FeO_{39}$ and $Bi_2Fe_4O_9$ not depending on the synthesis method [5-8]. The use of a mixture with a large excess of Bi_2O_3 also did not lead to a single-phase $BiFeO_3$ ferrite [9]. In [10] it is noted the difficulty of preparation of single-phase $BiFeO_3$, which is associated with the features of the system state diagram Bi_2O_3-Fe_2O_3 (the presence of three compounds), volatility Bi_2O_3 above the point of their melting point [11] and thermodynamic $BiFeO_3$ instability in air in the absence of $Bi2O_3$ equilibrium molten solution - Fe_2O_3 [12]. Analysis of the literature data shows the impossibility of obtaining a single-phase compound $BiFeO_3$ by solid-phase synthesis [13].

Thus existing thermal (solid-phase reaction at high temperatures (Tsin <Tm) and chemical (reaction solution) methods do not allow to obtain a single-phase ferrite bismuth. In this aspect, the scientific interest is the use of solar technology, i.e. synthesis of a melt obtained Exposure to concentrated high-density light radiation at which compounds are formed during reactions in melts, and then this state is fixed by quenching.

This work is aimed at studying the synthesis of $BiFeO_3$ from a mixture of bismuth (Bi_2O_3) oxides and iron (Fe_2O_3) fused on the solar furnace.

Methodology

At the first stage of the experiments, the oxides of bismuth (Bi_2O_3) and iron (Fe_2O_3) were melted on the focal plane of the solar furnace under the action of a concentrated light flux of 450 W / cm^2 density and held in the melting state for 15 minutes. The melts are quenched in water (104 deg / s). Molten melts in a ball mill by a wet method (material: water: grinding media = 1: 1: 1) for 10 hours. Sieved through a sieve of 0.05. On the basis of fused oxides, a mixture of Bi_2O_3 + Fe_2O_3 was produced in a stoichiometric ratio. Imagery-tablets are pressed by pressing at an effort of 1 ton on a C-100 press. The firing was carried out in an electric resistance furnace with silicate heaters at various temperatures. The samples were designated A-type.

***Corresponding author:** Paizullakhanov MS, Material science institute, Uzbekistan, Tashkent, Bodomzor street 2-B, Russia. E-mail: fayz@bk.ru

Received August 25, 2017; **Accepted** September05, 2017; **Published** September 19, 2017

Citation: Paizullakhanov MS (2017) $BiFeO_3$ Synthesized on the Solar Furnace. SF J Material Res Let 1:3.

In the second stage, bismuth ferrite was synthesized from a mixture of oxides without melting on a solar furnace (B-type samples) was used as control.

The thermogravimetric analysis of the Bi_2O_3 + Fe_2O_3 mixture was carried out in the temperature range 100-1000^{0}C on a Q-1500D derivatograph at a heating rate of 15^{o}C / min.

X-ray diffraction patterns were taken on powders using a DRON-3M diffractometer with copper anode. The determination of the apparent density of the samples, ρ, was carried out by hydrostatic weighing in octane, the calculation of the X-ray density, the ρent, was carried out according to the formula: ρrent = 1.66 × M / V (M weight of the formula unit in grams, V-volume of the perovskite cell in Å3) , Pot-on the formula (ρкж / ρрент) × 100%. The structural looseness was determined by the formula: ω = M / (nρ); Where M is the molecular weight equal to the sum of the atomic weights of the elements of the compound, n is the number of structural units (atoms, ions, complexes or radicals) in the formula unit of the compound, ρ is its density.

The coefficient of linear thermal expansion was determined on a cathetometer in the temperature range 25-600^{0}C. Micro structural studies were carried out on transparent (in transmitted light) and polished sections (in reflected light).

Results and Discussion

Figure 1 shows the differential-thermal analysis curve for the Bi_2O_3 + Fe_2O_3 mixture in the temperature range 100-1000^{0}C.

Figure 1: The Thermo Gravimetric Analysis of the Bi_2O_3 + Fe_2O_3 Mixture in the Temperature Range 100-1000^{0}C: a) with Components not Melted in the Solar Furnace, and b) With Components Melted in the Solar Furnace

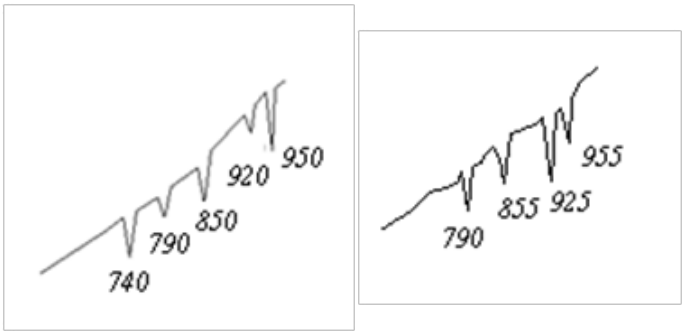

a) b)

The thermogravimetric analysis of the Bi_2O_3 + Fe_2O_3 mixture in the temperature range 100-1000^{0}C reveals 5 endothermic effects. It is clear that at 740^0 C a polymorphic Bi_2O_3 transformation occurs, the peak at 790^{0}C is due to the melting of the eutectic in the Bi_2O_3-Fe_2O_3 system at which the synthesis of $BiFeO_3$ begins. As the analysis of the DTA curve shows, $BiFeO_3$ begins to decompose at 920^{0}C and 950^{0}C. Analysis shows that on the DTA curve of a mixture of oxides melted on a solar furnace, there is no peak at 740^{0}C (Figure 1b). This indicates that the preliminary melting of the Bi_2O_3 and Fe_2O_3 components on a solar furnace leads to an increase in the chemical activity of the oxides. In addition, the endothermic peaks are shifted toward high temperatures by 50°C.

Figure 2 shows X-ray diffraction patterns of calcined samples at different temperatures.

An analysis of the X-ray diffraction pattern of the calcined sample at a temperature of 8850°C showed that this picture describes a $BiFeO_3$ compound with a rhombic lattice with lattice parameters a = 3.958, b = 3.78, c = 4.08 A (ITSM No. 20-169). There is also an impurity phase $Bi_2Fe_4O_9$ (solid $Fe_2O_32BiFeO_3$ solution) (ITSM No. 25-90).

Figure 2: The X-ray Diffraction Pattern of Bismuth Ferrite $BiFeO_3$ Synthesized at Various Temperatures (0C): a) 700; (B) 800; C) 885. X-phase Corresponds to a Solid Solution of $Bi_2Fe_4O_9$ = [Fe_2O_3 2$BiFeO_3$]

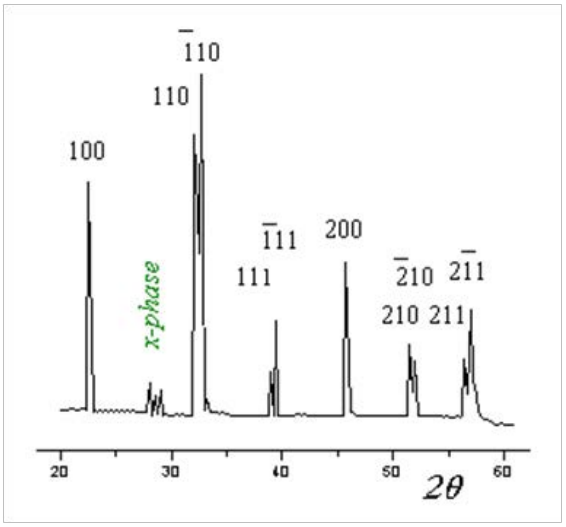

As is known, bismuth ferrite is characterized by orthorhombic distortion of the perovskite cell [18] and temperature-dependent non-stoichiometry [19, 20], which complicate the synthesis of single-phase bismuth ferrite, as well as compounds containing $BiFe0_3$.

The x-ray density of bismuth ferrite was ρ = 8.39 g / cm^3.

Figure 2 shows that, depending on the type of samples, the size and shape of the grains of ferrite of bismuth ceramics change. Thus, in the case of A-type samples, the grain size varies between 5-20 μm and 10-30 μm for B-type.

Table 1 shows the values of porosity, apparent density and coefficient of linear thermal expansion of the samples, depending on the synthesis method. It can be noted that the sinter ability of bismuth ferrite is somewhat improved when it is synthesized from fused oxides.

Figure 1(A&B): Microstructure of Bismuth Ferrite a) A- and b) B-types

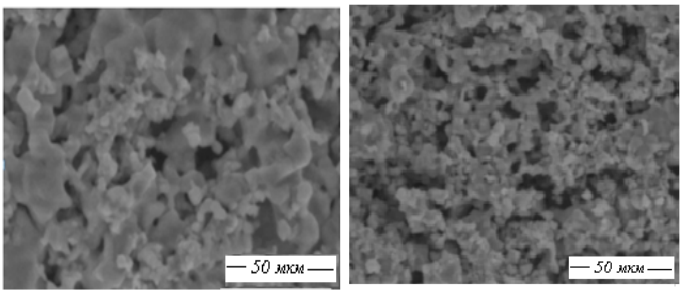

Table 1: The Values of Aparent Density (ρ density), Porosity (П), Relative Density (ρot), Structural Looseness (ω) and Coefficient of Linear Thermal Expansion (α) of Ceramic Bismuth Ferrite Samples, Depending on the History of the Components.

Samples	ρ, g/см^3	П, %	ρ_{arb}, %	ω	α.10^6, K^{-1}
A-type	5.40	36	64,36	7,36	13.4
B-type	4.87	42	58,04	11,44	11.9

The coefficient of linear thermal expansion was $13x10^{-6}K^{-1}$ for A-type samples with a predominance of rhombic phase and $11x10^{-6}K^{-1}$ for B-type samples in which the orthorhombic phase prevailed. The difference between the structural looseness of materials is due to the fact that preliminary melting of oxides on a solar furnace promotes the synthesis of bismuth ferrite with a denser structure.

Table 2 presents the results of the synthesis of bismuth ferrite as a function of the prehistory of the Fe_2O_3 and $Bi2O_3$ components. It can be seen that bismuth ferrite, obtained from fused oxides, is characterized by a small content of impurity phases. It can be assumed that the fused oxides are a more active form of the reagent, as a result of which the formation of impure $Bi_2Fe_4O_9$ begins at a lower temperature than the formation of bismuth ferrite.

Table 2: Results of Synthesis of Bismuth Ferrite as a Function of the Prehistory of Fe_2O_3 and Bi_2O_3 Components.

Prehistory of oxides Fe_2O_3 Bi_2O_3	Technological mode	Phase structure, %	
		$BiFeO_3$	$Bi_2Fe_4O_9$
Not melted on the solar furnace	885^0C, 5 h	88	12
Melted on the solar furnace		97	3

Thus, bismuth ferrite, synthesized on the basis of precursors - iron and bismuth oxides, melted on a solar furnace has a denser structure, a low coefficient of thermal expansion, in comparison with the traditionally synthesized bismuth ferrite. The technology of creating ceramic materials based on bismuth ferrite requires careful regulation of the physico-chemical state of the starting materials.

References

1. Paizullakhanov M (2016) Glass-crystalline materials of pyroxene composition. Comp Nanotechnol 2: 101-105.

2. Payzullakhanov M, Nurmatov Sh R, Shermatov Z (2013) Titanates of barium and strontium, synthesized in a field of concentrated light energy. Ceramica 9: 14-16.

3. Payzullakhanov M, Fayziev Sh A, Nurmatov Sh R, et al. (2013) Features of the synthesis of barium titanate in a field of concentrated light energy. Heliotechnics 4: 65-68.

4. Pyatakov AP, Zvezdin AK (2012) Magneto electric materials and multiferroics. Uspekhi Fizicheskikh Nauk 182: 593-620.

5. Catalan G, Scott JF (2009) Physics and Applications of Bismuth Ferrite. Advanced Materials 21: 2463-2485.

6. Khikhlovskyi VV (2012) The renaissance of multiferroics: bismuth ferrite ($BiFeO_3$) - a candidate multiferroic material in nanoscience.

7. Makoyed I (2009) Obtaining and physical properties of multiferroics: monograph. Brest: BrSU 181.

8. Morozov MI (2003) Features of the formation of $BiFeO_3$ in a mixture of bismuth and iron (III) oxides. J Gen Chem 73: 1772-1776.

9. Komandin GA (2010) Optical properties of $BiFeO_3$ ceramics in the frequency range 0.3-30 THz. Physics of the solid 52: 684-692.

10. Bernardo MS (2011) Reaction pathways in the solid state synthesis of multiferroic $BiFeO_3$. J Eur Ceram Soc 31: 3047-3053.

11. Kozakov AT, Guglev KA, Ilyasov VV (2011) Electronic structure of single-crystal ferrite of bismuth and hematite. FTT 53: 41-47.

12. Kazenas EK, Tsvetkov Yu V (2008) Thermodynamics of the evaporation of oxides. Moscow: LKI 480. Speranskaya EI, Skorikov VM, Rode E Ya, et al. (1965) The phase diagram of the bismuth oxide system is iron oxide, Izv. AN SSSR Ser Chemical 5: 905-906.

13. Filipyev VS, Smolyaninov NP, Fesenko EG, et al. (1990) Preparation of $BiFeO_3$ and determination of the unit cell. Crystallography 5: 958-959.

14. Fedulov SA, Venevtsev Yu N, Zhdanov GS (1961) High-temperature x-ray and thermo graphic studies of bismuth ferrite. Crystallography 6: 795-796.

15. Koizumi H, Nirizaki N, Ikeda T (1964) An X-ray Study on $Bi2O_3$-$Fe2O_3$ System. Jpn Appl Phys 495-496.

16. Morozov MI, Lomanova NA, Gusarov VV (2003) Features of the formation of $BiFeO_3$ in a mixture of oxides of bismuth and iron (III). Zhokh 73: 1772-1776.

Citation: Paizullakhanov MS (2017) $BiFeO_3$ Synthesized on the Solar Furnace. SF J Material Res Let 1:3.